Alzheimer β-Amyloid Peptide 25–35: Electrostatic Interactions with Phospholipid Membranes†

Evelyne Terzi,‡ Günter Hölzemann,§ and Joachim Seelig*,‡

Department of Biophysical Chemistry, Biocenter of the University of Basel, Klingelbergstrasse 70, CH-4056 Basel, Switzerland, and E. Merck, D-64271 Darmstadt, Germany

Received December 2, 1993; Revised Manuscript Received January 19, 1994®

ABSTRACT: The role of lipids in the aggregation of three Alzheimer model peptides was investigated with circular dichroism spectroscopy and high-sensitivity titration calorimetry under conditions of low ionic strength. In solution, the peptides βAP(25–35)OH and βAP(25–35Nle)NH_2 exhibit a reversible random-coil ⇄ β-sheet (or β-structured aggregate) transition. Addition of lipid vesicles containing negatively charged lipids shifts the random-coil ⇄ β-sheet equilibrium almost completely toward β-sheet structure, which can be explained by the specific conditions created at the membrane surface: the cationic peptides are attracted to the negatively charged membrane, and the increase in peptide concentration together with the partial alignment of the peptide molecules then facilitates β-sheet formation. The third peptide, βAP-(25–35)NH_2, also binds to the lipid membrane but was found to adopt an essentially random-coil structure, both with and without lipids. A quantitative characterization of the binding equilibrium was possible with high-sensitivity titration calorimetry. All three peptides exhibited exothermic binding enthalpies which varied between $\Delta H \approx -2$ kcal/mol for βAP(25–35)OH and −8 kcal/mol for βAP(25–35)NH_2. The apparent binding constants, calculated with bulk concentrations, were large and varied between 500 and 5×10^4 M^{-1}, depending on the experimental conditions. However, after correction for electrostatic charge effects using the Gouy–Chapman theory, the intrinsic binding constants were found to be constant and much smaller with $K \sim 2$–10 M^{-1}. The low intrinsic binding constants exclude significant hydrophobic interactions between the lipid membrane and the three Alzheimer model peptides even though residues 29–35 are considered to be part of a membrane-spanning domain in the full-length precursor protein. The predominance of electrostatic forces was demonstrated by addition of 0.1 M NaCl, which abolished the peptide–lipid interaction.

Alzheimer's disease, the degenerative disorder of the human brain, is characterized pathologically by abnormal depositions of protein in the brain. The major protein component is the β-amyloid peptide (βAP),[1] an amphiphilic peptide consisting of 39–43 amino acids. βAP is a proteolytic fragment of the membrane-bound β-amyloid precursor protein (βAPP) which is cleaved by an as yet unidentified protease (Kang et al., 1987). In βAPP, residues 1–28 of βAP constitute an extracellular domain whereas residues 29–39(43) form a transmembrane domain [cf. Fraser et al. (1991) and Selkoe (1993)]. No quantitative data exist on the binding of βAP itself to lipid membranes. Recently, βAP has been incorporated into phosphatidylserine liposomes, inducing the formation of Ca^{2+}-dependent channels when fused with planar lipid bilayers (Arispe et al., 1993). The role of the putative transmembrane domain is, however, unclear.

βAP fibrils are characterized by a high percentage of β-sheet structure whereas monomeric βAP adopts a predominantly random-coil conformation in solution [cf. Lansbury (1992), Barrow and Zagorski (1991), and Barrow et al. (1992)]. "Membrane-mimicking" solvents such as trifluoroethanol (TFE) have been found to induce either an α-helical structure or an oligomeric β-structure of βAP and also of some of its fragments (Barrow & Zagorski, 1991; Otvos et al., 1993), suggesting that similar conformational changes could be triggered upon interaction of βAP with lipid membranes. The relevance of these conformational transitions for membrane systems has, however, not been demonstrated experimentally.

We have previously shown that peptide βAP(25–35)OH in solution undergoes a concentration-dependent random-coil ⇄ β-sheet transition at pH 4.0 and 5.5 (Terzi et al., 1994). At pH 7.4, the equilibrium is shifted completely toward the β-sheet conformation whereas removal of the negative charge by amidation of the carboxy terminal stabilizes the random-coil conformation. A quantitative description of the random-coil ⇄ β-sheet transition was possible in terms of a simple cooperative association model. We have now investigated the influence of neutral and negatively charged lipid vesicles on the conformational equilibrium of βAP(25–35)OH and two related derivatives with CD spectroscopy and titration calorimetry. The selection of fragment βAP(25–35) for membrane binding studies is attractive for two reasons. On the one hand, βAP(25–35) comprises six amino acids of the putative transmembrane region which could be relevant for membrane binding. On the other hand, the C-terminal sequence of βAP(25–35)NH_2 (X-Gly-Leu-Met-NH_2) is identical to that of substance P and other tachykinin neuropeptides (Yankner et al., 1990). Since the binding of substance P to lipid membranes has been investigated in detail with various physical–chemical techniques (Seelig & Macdonald, 1989; Seelig, 1992), this facilitates quantitative comparison between the βAP fragments and substance P. The

† Supported by a FEBS long-term fellowship (E.T.) and by Swiss National Science Foundation Grant 31.27505.89.

‡ Biocenter of the University of Basel.

§ E. Merck.

® Abstract published in *Advance ACS Abstracts,* May 15, 1994.

[1] Abbreviations: POPC, 1-palmitoyl-2-oleoyl-*sn*-glycero-3-phosphocholine; POPG, 1-palmitoyl-2-oleoyl-*sn*-glycero-3-phosphocholine; AcO-Na, sodium acetate; MOPS, morpholinopropanesulfonic acid; TRIS, tris(hydroxymethyl)aminomethane; CD, circular dichroism; βAP, β-amyloid peptide; βAPP, β-amyloid precursor protein; SP, substance P; SUV, small unilamellar vesicle.

0006-2960/94/0433-7434$04.50/0 © 1994 American Chemical Society

amino acid sequences of substance P and of the synthetic βAP fragments used in this study are given below:

GSNKGAIIGLM-OH	βAP(25–35)OH
GSNKGAIIGLNle-NH_2	βAP(25–35Nle)NH_2
GSNKGAIIGLM-NH_2	βAP(25–35)NH_2
RPKPQQFFGLM-NH_2	substance P

The fragment βAP(25–35) has been reported to have the same neurotoxic and neurotrophic activities as the parent compound β(1–40) (Yankner et al., 1990). In addition, the amidated homologue βAP(25–35)NH_2, mimics the function of substance P (SP) on nicotine-evoked secretion and desensitization in adrenal chromaffin cells (Cheung et al., 1993). However, βAP(25–35)NH_2 was approximately 10-fold less effective than SP in protecting against nicotinic receptor desensitization. Moreover, βAP(25–35) did not bind to tachykinin receptors (Distefano et al., 1993; Burgevin et al., 1992; Lee et al., 1992). It was therefore of interest to establish the membrane binding properties of the various βAP(25–35) derivatives and to compare them with the known functional and physical–chemical properties of SP. Because of the low solubility of the above-mentioned peptides in physiological salt solutions, most experiments were made in 5 mM buffer without NaCl.

MATERIALS AND METHODS

Peptide Synthesis. βAP(25–35)OH was purchased from Saxon Biochemicals, Hannover, Germany. βAP(25–35)NH_2 was synthesized as described before (Terzi et al., 1994). βAP(25–35Nle)NH_2 was synthesized in a similar manner. In brief, the 9050 peptide synthesizer of Milligen was employed in the solid phase synthesis using the polyacrylamide resin derivatized with a Rink linker (Rink, 1987) and 9-fluorenylmethoxycarbonyl (Fmoc)-protected amino acids. After cleavage from the resin, the peptide was purified by chromatography on Sephadex G 10 and preparative HPLC. The purity and identity of the purchased and synthesized products were checked by analytical HPLC (better than 97% purity), NMR, FAB-MS, and amino acid analysis.

Circular Dichroism Spectroscopy. CD measurements were carried out on a Jasco J720 spectropolarimeter. All measurements were performed at room temperature. The path length of the quartz cell was 1 mm. All spectra were corrected by subtracting the buffer base line. Results are expressed in terms of mean residue ellipticity, $[\theta]_{MR}$, in units of deg cm^2 $dmol^{-1}$. CD measurements were performed at pH 4.0 and 5.5 using 5 mM sodium acetate buffer (NaOAc) and at pH 7.4 using 5 mM MOPS. Peptide solutions for CD measurements were prepared as described before (Terzi et al., 1994). For membrane binding studies, sonified unilamellar vesicles (SUV) of defined lipid composition were added to a buffered peptide solution and were measured after 10-min equilibration time.

Titration Calorimetry. Isothermal titration calorimetry was performed using an Omega MC-2 instrument from Microcal (Microcal, Northampton, MA) (Wiseman et al., 1989). All experiments were done at 28 °C. The experimental conditions were similar as described previously (Seelig & Ganz, 1991; Beschiaschvili & Seelig, 1992; Seelig et al., 1993). The preparation of sonified lipid vesicles followed the same procedure as described before (Seelig et al., 1993).

RESULTS

Lipid-Induced Conformational Changes As Detected by Circular Dichroism. CD spectra were recorded for βAP(25–35)OH, βAP(25–35)NH_2, and βAP(25–35Nle)NH_2, both with and without lipid vesicles.

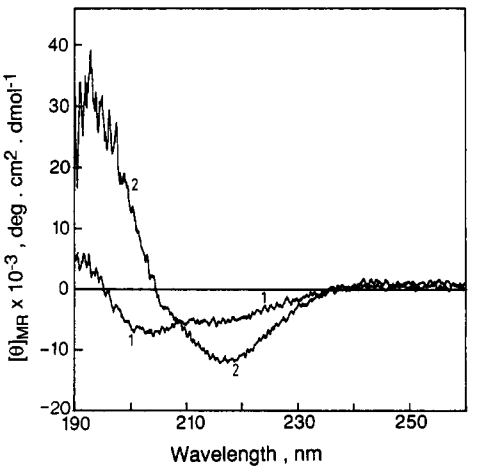

FIGURE 1: Lipid-induced random-coil ⇄ β-sheet transition of Alzheimer peptide fragment βAP(25–35)OH. Sonified unilamellar POPC/POPG vesicles (75:25 mol/mol) at a concentration of $C_{lipid} \approx 55$ mM were titrated into a 50 μM solution of βAP(25–35)OH (pH 5.0; 5 mM sodium acetate). The CD spectra correspond to different lipid-to-protein ratios. Curves: 1, 0; 2, 27.5.

βAP(25–35)OH in buffered solutions exhibits a concentration-dependent random-coil ⇄ β-sheet transition (pH 4.0–5.5). At low concentrations, the peptide adopts the random-coil conformation; at high concentrations, the equilibrium is shifted toward the aggregated state (predominantly β-sheet). The midpoint of the transition is at $c_{1/2} \approx 30$ μM, the association constant is $s = 2.9 \times 10^4$ M^{-1}, and the nucleation parameter is $\sigma = 0.2$. The maximum amount of β-sheet structure observed in the aggregates is $\beta_{max} \approx 70\%$ (Terzi et al., 1994).

Figure 1 then demonstrates the influence of lipids on this transition, measured at a peptide concentration of 50 μM and buffer of low ionic strength (5 mM sodium acetate buffer, pH 5.0). In the absence of lipid, the spectrum corresponds to approximately a 1:1 mixture of random-coil and β-sheet structure (spectrum 1). Addition of sonified POPC/POPG (75:25 mol/mol) vesicles has a dramatic effect on the CD spectrum: the equilibrium is shifted distinctly toward the β-structure (spectrum 2). In lipid-free solution, similar CD spectra could only be observed at much higher peptide concentrations; in fact, the addition of POPC/POPG vesicles is comparable to about an 5–8-fold increase in peptide concentration.

A similar behavior, both in pure buffer and with lipid vesicles, was encountered for βAP(25–35Nle)NH_2. The Nle residue, an isosteric replacement of the Met residue, is known to favor β-sheet structure (Arfmann et al., 1977) and thus appeared to be a good candidate for a substitution in which the β-structure was to be retained. First experiments at pH 4.0 and 5.5 [i.e., in the pH range of the βAP(25–35)OH transition] were nevertheless unsuccessful since the peptide was found in a predominantly random-coil conformation up to $C_{pep} \sim 400$ μM. However, increasing the pH to 7.4 led to a concentration-dependent conformational transition with an isodichroic point at 200 nm as illustrated in Figure 2. At high concentrations, the CD spectrum revealed some type of β-structure [cf. Hollosi et al. (1985)], whereas upon dilution the molecule adopted a random-coil conformation.

In order to detect the formation of aggregates, a 0.5 mM peptide solution (exhibiting a CD spectrum with mainly β-structure) was filtered through a Millipore filter (0.22-μm pore size). The filtrate gave rise to a random-coil-type CD spectrum with an ellipticity corresponding to a peptide

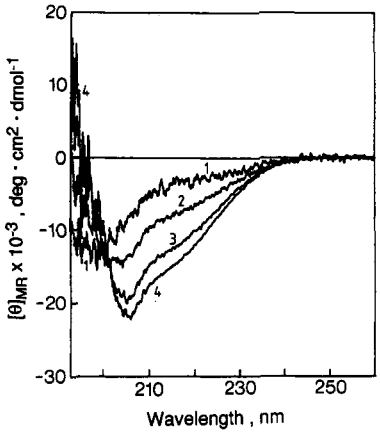

FIGURE 2: Alzheimer peptide fragment βAP(25–35Nle)NH_2. CD spectra were recorded as a function of peptide concentration (5 mM MOPS, pH 7.4). The CD spectra were generated by diluting a 1 mM stock solution. The peptide concentrations corresponding to the different CD spectra are as follows: curve 1, 50 μM; 2, 167 μM; 3, 250 μM; 4, 400 μM. The spectra indicate a β-structure → random-coil-type transition upon dilution.

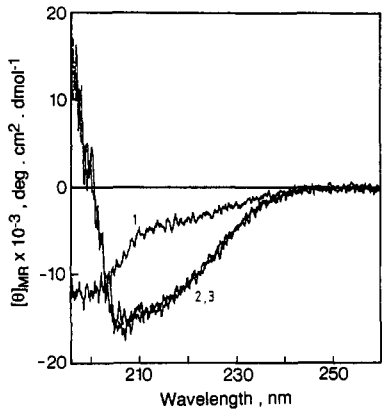

FIGURE 3: Lipid-induced random-coil → β-structure transition of the Alzheimer peptide fragment βAP(25–35Nle)NH_2. Peptide concentration, 100 μM. Different amounts of POPC/POPG vesicles (75:25 mol/mol) were added to the peptide stock solution. The CD spectra provide evidence for a distinct increase in β-structure upon lipid addition. The different spectra correspond to different molar lipid-to-protein ratios: curve 1, 0; curve 2, 2.75; curve 3, 5.5 (5 mM MOPS buffer, pH 7.4).

concentration of ~0.3 mM; 40% of the initial amount of peptide was retained by the filter. βAP(25–35Nle)NH_2 thus behaves similar to βAP(25–35)OH and also exhibits a concentration-dependent aggregation which is reversible upon dilution. The midpoint of the transition is found at about $c_{1/2} \approx 150$ μM, and a quantitative analysis of the transition equilibrium is possible using the association model described for βAP(25–35)OH (Terzi et al., 1994). An association constant of $s = 1.2 \times 10^4$ M^{-1} and a nucleation parameter of $\sigma = 0.01$ are derived, which are in broad agreement with the corresponding parameters determined for βAP(25–35)OH.

Next, CD spectra of βAP(25–35Nle)NH_2 were recorded in the presence of lipid vesicles, and the results are shown in Figure 3. Addition of negatively charged POPC/POPG vesicles led to an increase in β-structure (no ellipticity minimum was detected at 222 nm); neutral vesicles had no effect. It should be noted, however, that the CD spectra of βAP(25–35Nle)NH_2 are different from those obtained with βAP(25–35)OH, indicating subtle differences in secondary structure. Nevertheless, the conformational behavior of the two synthetic peptides in the presence of lipids is rather similar.

The third peptide studied, βAP(25–35)NH_2, bears a close resemblance to SP since the C-termini of the two molecules

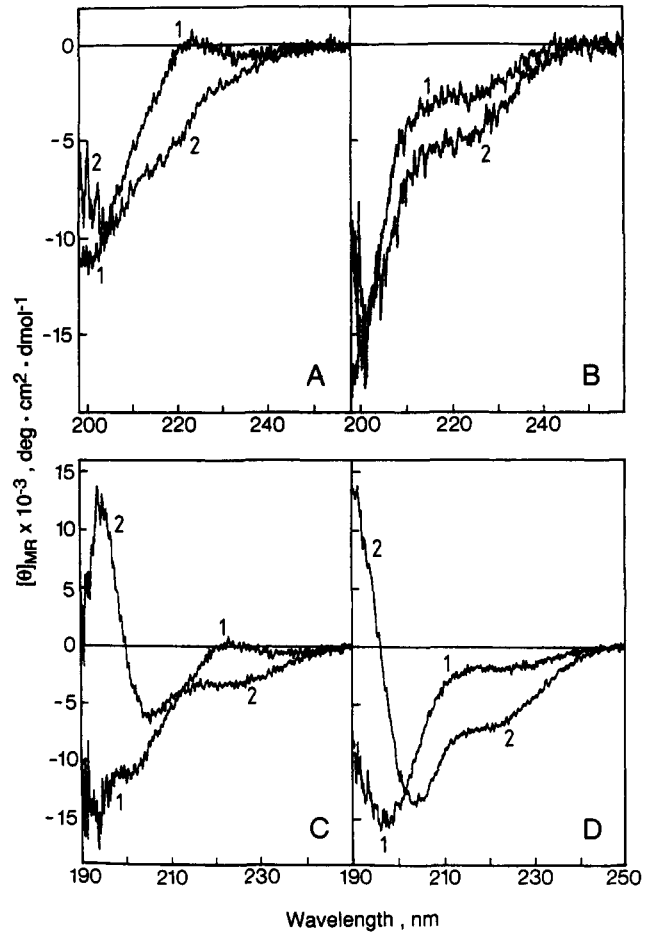

FIGURE 4: CD spectra of substance P (SP) and the Alzheimer peptide βAP(25–35)NH_2 in the presence of phospholipid vesicles and in TFE/water mixtures. (A) SP in buffer (curve 1) and with POPC/POPG vesicles (curve 2; lipid-to-protein ratio 13.75). (B) βAP(25–35)-NH_2 in buffer (curve 1) and with POPC/POPG vesicles (curve 2; lipid-to-protein ratio 18.3). (C) SP in buffer (curve 1) and in TFE/buffer (curve 2; TFE/water 50:50 v/v). (D) βAP(25–35)NH_2 in buffer (curve 1) and in TFE/buffer (curve 2; TFE/water 50:50 v/v). c_{pep} = 100 μM; vesicle composition POPC/POPG 75:25 mol/mol; buffer composition, 5 mM MOPS, pH 7.4. The spectra in buffer are characteristic of a predominantly random-coil conformation. In the presence of lipid, the conformational changes are small whereas TFE induces a distinct increase in α-helical structure.

are identical. CD spectra of βAP(25–35)NH_2 and SP are compared in Figure 4. In the absence of lipid, both peptides exhibit CD spectra which are typical for a random-coil conformation. Addition of sonified POPC/POPG vesicles (75:25 mol/mol) to SP (Figure 4A) or βAP(25–35)NH_2 (Figure 4B) leads to only small conformational changes which for SP is in agreement with the earlier literature [cf. Rolka et al. (1986) and Williams and Weaver (1990)]. Pure POPC vesicles have no effect on both peptides. The weak lipid effect is in sharp contrast to distinct conformational changes induced by trifluoroethanol (TFE), a "membrane-mimicking" solvent. The CD spectra of SP (Figure 4C) and βAP(25–35)NH_2 (Figure 4D) in buffer containing 50% TFE are characterized by large contributions of α-helical structure (minima at 206 and 222 nm) and hence are different from those obtained with lipid vesicles [cf. Rolka et al. (1986) for SP in the presence of TFE]. Self-association of SP has been observed only at pH 3 and high peptide concentrations (1–10 mM). Under these conditions, the corresponding CD spectra suggest the formation of β-ordered structures (Rueger et al., 1984).

The requirement for negatively charged lipids to induce a conformational change in the βAP derivatives suggests that

the dominant factor in membrane binding is the electrostatic attraction of the positively charged peptides to the negatively charged membrane surface. This was further investigated with titration calorimetry.

Titration Calorimetry. A quantitative characterization of the peptide–membrane binding equilibrium was possible with high-sensitivity titration calorimetry. The method can be applied in two different modes. (1) Injection of peptide into a large excess of lipid (under conditions of complete peptide binding) allows the immediate evaluation of the binding enthalpy ΔH. (2) In the second mode, the reverse titration is performed; i.e., lipid veicles are injected into a diluted peptide solution. Each injection entails a heat of reaction. Δh_i, as the peptide binds to the outer leaflet of the lipid vesicle. However, the heat of reaction is not constant as in mode 1 but decreases gradually as less and less peptide is available for binding. From the cumulative heat after i injection steps, $\sum \Delta h_i$, the degree of binding, $X_b^{(i)}$, can be calculated. Furthermore, the cumulative heat at the end point of the titration yields again the binding enthalpy, ΔH, and, more important, from the shape of the titration curve, the binding constant, K, can be derived (Beschiaschvili & Seelig, 1992; Seelig et al., 1993).

We first discuss titration calorimetry experiments with βAP-(25–35)NH_2 for which CD spectroscopy revealed only a small conformational change upon addition of negatively charged SUVs. Surprisingly, injection of this peptide into a suspension of the same vesicles in the titration calorimeter produced a considerable exothermic heat of reaction with $\Delta H \approx -7.5 \pm 1.1$ kcal/mol (data not shown). Apparently, the peptide interacts strongly with the negatively charged membrane, even though the CD-detectable conformational change is small. The control experiment, injection of βAP(25–35)NH_2 into buffer (5 mM MOPS, pH 7.4), yielded a dilution enthalpy of $\Delta H \approx +0.8$ kcal/mol while the dilution of lipid vesicles with buffer produced no heat effect at all. After correction for the dilution effect, the total heat of binding of βAP(25–35)NH_2 to POPC/POPG SUVs was $\Delta H \approx -8.3$ kcal/mol. A peptide-induced vesicle fusion can be excluded on grounds that (i) the heat evolvement is rapid and (ii) the base line remains smooth and stable during the whole titration experiment.

The binding constant of the βAP(25–35)NH_2–membrane equilibrium was determined by the experiment displayed in Figure 5A where sonified POPC/POPG vesicles were injected into a 50 μM peptide solution. Each injection (10 μL) of the negatively charged lipid vesicles (55 mM) caused an exothermic heat of reaction with the peak height decreasing smoothly as the amount of *free* peptide became continuously reduced (Figure 5A). The cumulative heat of reaction is summarized in Figure 5B. From the end point of the titration, a reaction enthalpy of $\Delta H = -7.7$ kcal/mol is evaluated, in agreement with the above peptide → lipid experiment. The solid line in Figure 5B represents the theoretical analysis of the binding isotherm using the same model as employed for the binding of other peptides such as melittin or somatostatin to lipid membranes (Beschiaschvili & Seelig, 1992; Seelig et al., 1993). The model assumes (i) an electrostatic attraction of the positively charged peptide to the membrane, (ii) a "chemical" (or "hydrophobic") binding step from the surface layer with increased peptide concentration to the plane of binding, and (iii) a change in protonation of the N-terminal amino groups as the peptide moves from bulk solution with pH 7.4 to the more acidic membrane surface (pH ~ 5.5) (cf. below). The theoretical curve in Figure 5B was calculated with an intrinsic (or chemical) binding constant of $K = 2$ M^{-1}

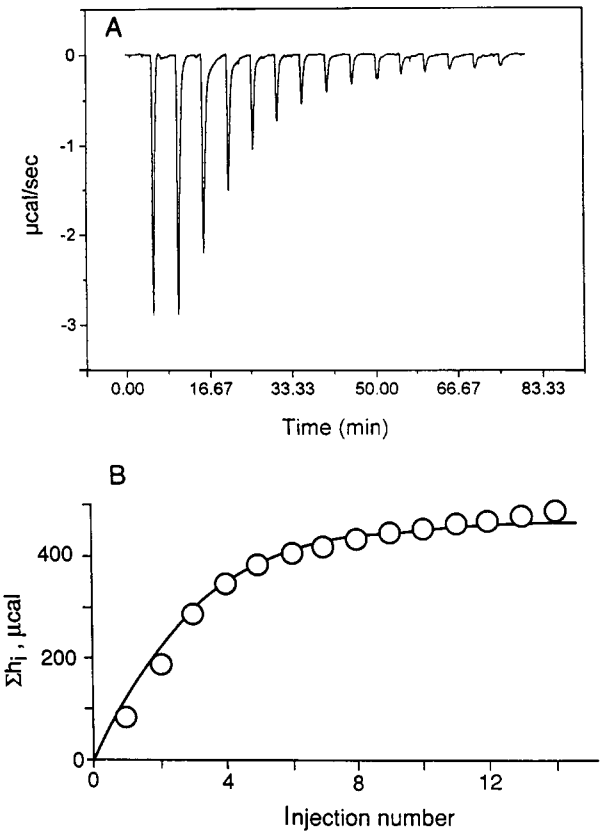

FIGURE 5: Titration calorimetry of βAP(25–35)NH_2 ($c_{pep} = 50$ μM) with small unilamellar lipid vesicles (lipid composition POPC/POPG 75:25 mol/mol). Concentration of lipid vesicles $C_{lip} \approx 55$ mM. Only the outer leaflet (~60% of total lipid) is involved in peptide binding. Measurement at 28 °C, pH 7.4, in 5 mM MOPS buffer. (A) Each peak corresponds to the injection of 10 μL of sonified SUVs dispersed in the same buffer as the peptide solution. (B) Cumulative heat of reaction as a function of the number of injections. The solid line was calculated with an intrinsic binding constant of $K = 2$ M^{-1} and a binding enthalpy of $\Delta H = -7.7$ kcal/mol. Electrostatic effects were taken into account by means of the Gouy–Chapman theory.

and a pK value of 7.2 for the N-terminal amino group, leading to an effective electric charge at the membrane surface of $z = +2$. The binding constant K refers to a surface partition equilibrium according to

$$X_b = Kc_I \quad (1)$$

where X_b is the molar amount of peptide bound per mole of total phospholipid and c_I is the peptide concentration in the interfacial layer (Seelig et al., 1993). c_I is distinctly larger than the peptide concentration in bulk solution, c_{eq}, and can be calculated by combining the Boltzmann equation with the Gouy–Chapman theory. The advantage of this binding model is that it allows a separation of electrostatic effects from the "chemical" binding step.

The major role of electrostatics in the present binding experiments is, in part, due to the *low ionic strength* (5 mM MOPS buffer) of the medium. Under these conditions, the surface of a POPC/POPG (75:25 mol/mol) membrane is characterized by a potential of about −120 mV, and the concentration of the cationic βAP(25–35)NH_2 peptide with $z = +2$ is about 2000-fold higher at the interface than in solution. The low intrinsic binding constant of $K = 2$ M^{-1} is thus more than compensated for by the high peptide concentration at the interface.

The influence of electrostatic attraction was tested by repeating the above titration experiment in the presence of 10

or 100 mM NaCl. At 10 mM NaCl concentration, distinctly smaller heats of reaction were observed than those shown in Figure 5. However, after using the Gouy–Chapman theory to correct for the increased ionic screening, almost the same intrinsic binding constant of $K = 3\ M^{-1}$ was evaluated. The binding enthalpy was reduced to $\Delta H \approx -2.3$ kcal/mol. Increasing the NaCl concentration even further to 0.1 M NaCl completely abolished the binding, and no heat of reaction could be measured (data not shown). βAP(25–35)NH_2 was also injected into a dispersion of neutral POPC vesicles. No heat of reaction was observed, providing further evidence for the dominant role of electrostatic interactions.

Analogous titrations were performed with the norleucine-containing peptide βAP(25–35Nle)NH_2. Addition of this peptide to an excess of sonified, unilamellar POPC/POPG vesicles produced an exothermic heat of reaction with $\Delta H \approx -3.5$ kcal/mol. The control experiment, i.e., the injection of the same peptide solution into buffer, yielded an endothermic heat of dilution of about $\Delta H_{dil} \sim +1.0$ kcal/mol. The corrected binding enthalpy of peptide βAP(25–35Nle)NH_2 to POPC/POPG SUVs at pH 7.4 and 5 mM MOPS is thus $\Delta H \approx -4.5 \pm 0.5$ kcal/mol. No binding enthalpy was measured for pure POPC vesicles.

Since the peptide concentration in the injection syringe was 500 μM, addition of 10 μL of this solution to a calorimeter cell of $V \sim 1$ mL produced an initial peptide concentration of only ~ 5 μM. At a concentration of 500 μM, the peptide is aggregated, adopting an essentially β-type conformation; at 5 μM, the equilibrium is shifted toward the monomeric random-coil structure (cf. Figure 2). The dilution experiment, however, demonstrates that the conformational transition is associated with only a small enthalpy change of $\Delta H \approx +1.0$ kcal/mol.

We have also investigated the inverse type of reaction; i.e., negatively charged lipid vesicles ($c_{lipid} \approx 55$ mM) were injected into a 50 μM βAP(25–35Nle)NH_2 solution (pH 7.4, 5 mM MOPS). The heat of reaction decreased continuously with each injection step, and from the end point of the titration, the total binding enthalpy was calculated as $\Delta H \approx -4.4$ kcal/mol, in agreement with the data mentioned above. From the shape of the titration curve, an intrinsic binding constant of $K = 3.8\ M^{-1}$ could be derived, electrostatic effects being accounted for by the Gouy–Chapman theory (effective peptide charge at the membrane surface $z \approx +2$).

We finally discuss the behavior of βAP(25–35)OH in the presence of lipid membranes. Again, two different processes appear to contribute to the measured heat of reaction, ΔH, namely (i) the aggregation $\rightleftarrows$ dissociation reaction of the peptide itself and (ii) the binding of the peptide to the lipid membrane. The dissociation enthalpy of βAP(25–35)OH can be determined by injecting a concentrated peptide solution (e.g., 0.5 mM) into the calorimeter cell filled with buffer only. Such dilution experiments were performed at pH 4.0 and 5.0 since CD spectroscopy revealed a β-sheet $\rightleftarrows$ random-coil transition under these conditions (Terzi et al., 1994). The dilution enthalpy, ΔH_{dil}, was again endothermic, as observed for βAP(25–35Nle)NH_2, but considerably larger. It decreased from $\sim +3.0$ kcal/mol in the first injection to $\sim +2.0$ kcal/mol at the end of the measurement ($c_{pep} = 0.5$ mM). We have repeated such dilution experiments under a variety of conditions (peptide concentrations 0.25–2.0 mM; pH 4.0, 4.5, 5.0; injection volumes ranging between 10 and 250 μL) and observed similar *endothermic* dilution enthalpies of $\Delta H_{dil} \approx$ 1–3 kcal/mol in all experiments.

In contrast, *exothermic* heats of reaction were measured in lipid binding experiments, i.e., when a solution of βAP(25–35)OH was injected into a suspension of POPC/POPG vesicles (no effect with pure POPC vesicles). In a typical experiment with negatively charged POPC/POPG SUVs, the reaction enthalpy was found to be $\Delta H \approx -3.3$ kcal/mol (pH 5.0; 5 mM AcONa buffer). In the inverse experiment [POPC/POPG vesicles injected into a 50 μM solution of βAP(25–35)OH, pH 5.0, and 5 mM AcONa], the reaction enthalpy was smaller (-1.4 kcal/mol $> \Delta H > -1.9$ kcal/mol), and an intrinsic binding constant of $K \sim 10\ M^{-1}$ was derived, suggesting again electrostatic attractions as the main binding force for this peptide. An effective charge of $z = 1.5$ had to be used in this calculation since the two positive charges at the N-terminus are partially compensated by the negative charge of the carboxy terminus. However, the quality of the theoretical fit to the experimental data was less satisfactory than for the other two peptides, presumably due to interference between dissociation and binding reactions.

DISCUSSION

Random-Coil $\rightleftarrows$ β-Sheet Transition in Solution. The synthetic peptides βAP(25–35)OH, βAP(25–35)NH_2, and βAP(25–35Nle)NH_2 serve as model systems for the full-length Alzheimer peptide βAP(1–40)OH. The latter exhibits a low solubility under physiological conditions and easily forms aggregates (fibrils) characterized by a high percentage of β-sheet structure (Barrow & Zagorski, 1991). Fibril formation has also been observed for two of the above model peptides, namely, βAP(25–35)OH (Terzi et al., 1994) and the norleucine derivative βAP(25–35Nle)NH_2 (this work). For both peptides, the aggregation process was found to be a reversible, concentration-dependent phenomenon; dilution of concentrated samples generated CD spectra with increasing percentage of random-coil structure.

Molecular modeling studies of βAP(25–35)OH suggest an antiparallel β-pleated sheet structure with ion pair formation between the carboxy terminus of Met-35 and the $-NH_3^+$ group of Lys-28 (Terzi et al., 1994). For geometrical reasons, residues 25–27 cannot be involved in direct interchain contacts, and the maximum amount of β-structure appears to be 70%, in agreement with the CD data.

Ion pair formation is not possible for βAP(25–35Nle)NH_2 due to its amidated carboxy terminus. Electrostatic interactions are replaced by enhanced van der Waals contacts via the norleucine residue, a well-known β-structure promoter (Arfmann et al., 1977). The important role of the Nle-35 residue becomes obvious if βAP(25–35Nle)NH_2 is compared with the closely related peptide βAP(25–35)NH_2: fibril formation is not observed for the latter. SP, finally, exhibits a CD spectrum similar to that of βAP(25–35)NH_2 (with even more random-coil contribution) and also shows no tendency of fibril formation under the present experimental conditions.

The energetic contributions of ion pair formation and van der Waals contacts toward β-sheet formation appear to be roughly equivalent if the aggregation is analyzed in terms of the linear association model (Terzi et al., 1994). The two aggregation equilibria are characterized by similar association constants of $s = 2.9 \times 10^4\ M^{-1}$ for βAP(25–35)OH (Terzi et al., 1994) and $s = 1.2 \times 10^4\ M^{-1}$ for βAP(25–35Nle)NH_2 (this work). On the other hand, the nucleation step is found to be more difficult for βAP(25–35Nle)NH_2 with $\sigma = 0.01$ than for βAP(25–35)OH with $\sigma = 0.2$. This suggests that the long-range electrostatic interactions between the carboxylic group of Met-35 and the $-NH_3^+$ end of Lys-28 are more

efficient in inducing the correct β-sheet alignment than the short-range van der Waals interactions.

It should be noted that the CD spectra of the two peptides are not identical in the aggregated state, suggesting that slightly different types of β-structures are formed by the two molecules. The isodichroic points for the random-coil ⇄ β-sheet (β-structured aggregate) transition are also different with λ = 206 nm for βAP(25–35)OH and λ = 200 nm for βAP(25–35Nle)NH_2.

Thermodynamics of Lipid–Peptide Interactions. The exothermic heats of reaction measured with titration calorimetry provide evidence that all three peptide fragments interact with lipid vesicles. The presence of negatively charged lipids is a prerequisite for peptide binding since no reaction enthalpies were detected with electrically neutral phosphatidylcholine membranes. Moreover, the binding to the negatively charged membrane could be abolished by applying high concentrations of NaCl [0.1 M NaCl; only βAP(25–35)NH_2 investigated].

As mentioned above, the binding process can be divided into two steps. The first is an electrostatic attraction of the positively charged peptide toward the membrane surface; the second is the binding step proper. The electrostatic attraction leads to an increase in peptide concentration in the lipid–water interface. The interfacial concentration, C_I, is related to the equilibrium concentration in bulk solution, C_{eq} according to

$$C_I = C_{eq} \exp(-zF_0\psi_0/RT) \quad (2)$$

where z is the effective charge of the peptide, F_0 is the Faraday constant, and RT is the thermal energy. The membrane surface potential, ψ_0, is not measurable but can be calculated by means of the Gouy–Chapman theory (Aveyard & Haydon, 1973; McLaughlin, 1977, 1989). The second step in the binding process is the transition from the interfacial layer to the lipid membrane. Several models are possible to describe this "chemical" binding step. The simplest approach is to assume a surface partition equilibrium as defined by eq 1, but more complicated models such as the Langmuir adsorption isotherm with only a limited number of binding sites are equally possible.

In many biochemical studies, no distinction is made between bulk solution and interfacial layer, and binding equilibria are described in terms of bulk concentrations only. For comparative purposes, we therefore define an apparent binding constant, K_{app}, according to

$$X_b = K_{app}C_{eq} \quad (3)$$

which is related to the intrinsic binding constant as

$$K_{app} = K \exp(-zF_0\psi_0/RT) \quad (4)$$

Equation 4 demonstrates that K_{app} is not truly constant but will vary as a function of the membrane surface potential and, in turn, the peptide concentration. For the present experimental conditions, $C_{eq} \ll C_I$ and hence $K_{app} \gg K$.

The negative membrane surface potential not only attracts cationic peptides but also attracts Na^+ and H^+. Both effects have been taken into account in the present analysis. For Na^+ ions, a binding constant $K = 0.6$ M^{-1} was used, and the screening of the surface charge by Na^+ was calculated with a Langmuir adsorption isotherm (Macdonald & Seelig, 1987; Seelig et al., 1993). The change in pH was evaluated from the surface potential ψ_0 using again the Boltzmann relation.

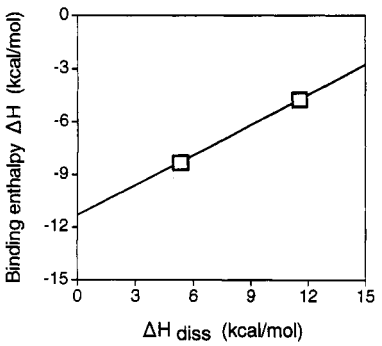

FIGURE 6: Variation of the binding enthalpy of βAP(25–35)NH_2 with the buffer dissociation enthalpy. Each data point corresponds to at least two independent measurements which were made at pH 7.4 with either 5 mM TRIS (ΔH_{Diss} = 11.51 kcal/mol) or 5 mM MOPS (ΔH_{Diss} = 5.29 kcal/mol). The binding reaction was recorded for sonified POPC/POPG (75:25 mol/mol) vesicles. Temperature 28 °C.

Under the present experimental conditions (25% POPG, low ionic strength), the pH decreases smoothly from pH 7.4 in bulk solution to pH 5.5 at the membrane surface. The pH shift entails a protonation of the amino terminus as the peptide approaches the membrane. Assuming a pK value of 7.2 for the amino-terminal NH_2 group [cf. Seelig (1990)], the extent of protonation in bulk solution is only 38%, but increases to almost 100% near the more acidic membrane surface.

The proton uptake could be confirmed experimentally by measuring the binding enthalpy in two buffers of different dissociation enthalpy. In Figure 6, the measured ΔH values of βAP(25–35)NH_2 are plotted versus the buffer dissociation enthalpy. The slope of the straight line is $n = 0.57$, indicating an uptake of 0.57 mol of protons per mole of bound peptide. Within the accuracy of the measurement, this is in agreement with the above theoretical prediction of 0.62. The reaction enthalpy measured in TRIS buffer (ΔH = –4.8 kcal/mol) can be considered to be the *intrinsic* binding enthalpy of peptide βAP(25–35)NH_2 since the proton donor (NH_3^+ group of TRIS) and the proton acceptor [NH_2 group of βAP(25–35)-NH_2] have approximately similar dissociation/association enthalpies of ~11 kcal/mol [cf. Martin (1964) and Seelig et al. (1993)].

For all three model peptides, the intrinsic binding constant K (which is independent of the electrostatics at the membrane surface) was found to be in the range of 1–10 M^{-1} whereas the apparent binding constants were much larger (K_{app} ~ 500–50 000 M^{-1}) and strongly dependent on the experimental conditions. From the large discrepancy between the apparent and the intrinsic binding constant, it can be concluded that the binding of the three model peptides to the lipid membrane is driven essentially by electrostatic attractions.

A similar result was obtained previously for substance P based on a completely different experimental approach. Using the monolayer method and choosing film conditions typical for a lipid bilayer (lateral film pressure of ~32 mN/m), SP binding was measured via the area increase of the monolayer upon peptide penetration. Negatively charged lipids were required for SP binding. The apparent binding constant was of the order of 10^4 M^{-1} whereas the intrinsic binding constant was evaluated as $K \approx 1$ M^{-1} (Seelig & Macdonald, 1989).

All four peptides exhibit only small intrinsic binding constants, attesting to a rather weak hydrophobic binding. The corresponding free energies of binding, calculated according to $\Delta G = -RT \ln(55.5\ K)$, are in the range of –2.4 to –3.5 kcal/mol. [The factor 55.5 corrects for the cratic contribution in the surface partition equilibrium; cf. Cantor

and Schimmel (1980).] Surprisingly, the corresponding binding enthalpies vary considerably between −8 and −2 kcal/mol. Even though the binding is mainly enthalpy-driven, the constancy of the free energy of binding suggests an entropy–enthalpy compensation mechanism to be effective. The molecular origin of this phenomenon is unclear, but entropy–enthalpy compensation mechanisms are quite common in other fields of chemistry, most notably in the host–guest complexation mechanism [cf. Smithrud et al. (1991) and Inoue et al. (1993) for recent examples].

Role of the Membrane Surface in the Random-Coil ⇄ β-Sheet Equilibrium. For all peptides studied, the binding to the lipid membrane was accompanied by a conformational change which was small for βAP(25–35)NH_2 and SP (Figure 4), but quite large for βAP(25–35)OH (Figure 1) and βAP-(25–35Nle)NH_2 (Figure 3).

A structural interpretation of the CD spectra was difficult for βAP(25–35)NH_2 and SP. However, when the same peptides were dissolved in TFE/water mixtures, the CD spectra showed a large increase in α-helix content and were different from those obtained in the presence of lipid vesicles (Figure 4). As far as TFE mimics a hydrophobic environment, these results suggest that the two peptides do not penetrate into the hydrophobic part of the lipid bilayer.

The most conspicuous results were obtained, however, for βAP(25–35)OH (at pH 5.0) and βAP(25–35Nle)NH_2 (at pH 7.4), where the addition of negatively charged vesicles shifted the equilibrium transition from random coil to a β-sheet, reversing the effect of the dilution experiment (Figure 2). The CD spectra were similar to those measured at high peptide concentration in the absence of lipid and were different from those measured in TFE/water mixtures [at least for βAP-(25–35)OH]. Taken together, the data argue against lipid penetration of the two peptides but suggest a new type of lipid–protein interaction, namely, a *lipid-induced peptide aggregation* at the membrane surface: the lipid membrane attracts cationic peptide to its negatively charged surface, creating, at the same time, a parallel alignment of the peptide chains. The ordering of the peptide chains together with the increased peptide concentration at the interface greatly facilitates β-sheet (β-structured aggregate) formation. The role of the membrane surface is then 2-fold. On the one hand, it may act as a catalyst, reducing the activation energy for the correct positioning of the peptide chains. On the other hand, the membrane truly shifts the thermodynamic equilibrium, favoring β-sheet formation via increased interfacial peptide concentration. Secondary structure formation as a consequence of aggregation has been also demonstrated for other peptide systems [cf. Mutter and Hersperger (1990)].

Conclusions. Under conditions of low ionic strength, the Alzheimer peptides βAP(25–35)OH and βAP(25–35Nle)-NH_2 undergo a concentration-dependent and reversible random-coil ⇄ β-sheet (β-structured aggregate) transition which can be described quantitatively by a linear association mechanism. The two peptides also establish model systems for a lipid-induced peptide aggregation since the addition of negatively charged lipids shifts the equilibrium toward β-structure. This behavior can be explained by an increase of the peptide concentration at the membrane surface due to electrostatic attractions. Two other peptides, βAP(25–35)-NH_2 and the related neuropeptide SP, retain an essentially random-coil conformation under similar conditions and are little affected by the addition of lipid. The lipid binding can be quantitated with high-sensitivity titration calorimetry since all three Alzheimer peptides exhibit exothermic binding enthalpies, albeit of different magnitude. Referred to the peptide concentration at the membrane surface, i.e., the concentration immediately above the plane of binding, the binding mechanism follows a surface partition equilibrium with intrinsic binding constants of about 2–10 M^{-1}, providing evidence for only weak hydrophobic interactions between the three model peptides and the bilayer membrane. The overall binding constants which include the electrostatic attraction toward the membrane surface are 2–3 orders of magnitude larger and furthermore concentration-dependent. The electrostatic interactions are abolished in 0.1 M NaCl as evidenced by the loss of ΔH effects.

ACKNOWLEDGMENT

We are indebted to Dr. Anna Seelig for stimulating discussions and helpful suggestions. We thank Ms. Sandra Lotz for carefully reading the manuscript.

REFERENCES

Arispe, N., Rojas, E., & Pollard, H. B. (1993) *Proc. Natl. Acad. Sci. U.S.A. 90*, 567–571.

Artmann, H. A., Labitzke, R., & Wagner, K. G. (1977) *Biopolymers 16*, 1815–1826.

Aveyard, R., & Haydon, D. A. (1973) *An Introduction to the Principles of Surface Chemistry*, Cambridge University Press, London.

Barrow, C. J., & Zagorski, M. G. (1991) *Science 253*, 179–182.

Barrow, C. J., Yasuda, A., Kenny, P. T. M., & Zagorski, M. G. (1992) *J. Mol. Biol. 225*, 1075–1093.

Beschiaschvili, G., & Seelig, J. (1992) *Biochemistry 31*, 10044–10053.

Burgevin, M. C., Daniel, N., Doble, A., & Blanchard, J. C. (1992) *Neuroreport 3*, 1131–1134.

Cantor, C. R., & Schimmel, P. R. (1980) *Biophysical Chemistry*, Vol. I, p 283 W. H. Freeman, San Francisco.

Cheung, N. S., Small, D. H., & Livett, B. G. (1993) *J. Neurochem. 60*, 1163–1166.

Distefano, M. Aleppo, G., Casabona, G., Genazzani, A. A., Scapagnini, U., & Nicoletti, F. (1993) *Brain Res. 600*, 166–168.

Fraser, P. E., Nguyen, J. T., Surewicz, W. K., & Kirschner, D. A. (1991) *Biophys. J. 60*, 1190–1201.

Hollosi, M., Kawai, M., & Farman, G. D. (1985) *Biopolymers 24*, 211–242.

Inoue, Y., Hakushi, T., Liu, Y., Tong, L.-H., Shen, B.-J., & Jin, D.-S. (1993) *J. Am. Chem. Soc. 115*, 475–481.

Kang, J., Lemaire, H.-G., Unterbeck, A., Salbaum, J. M., Masters, C. L., Grzeschik, K.-H., Multhaup. G., Beyreuther, K., & Müller-Hill, B. (1987) *Nature 325*, 733–736.

Lanbury, P. T. (1992) *Biochemistry 31*, 6865–6870.

Lee, J. M., Weinstein, D. A., Kowall, N. W., & Beal, M. F. (1992) *Drug Dev. Res. 27*, 441–444.

Macdonald, P. M., & Seelig, J. (1987) *Biochemistry 26*, 1231–1240.

Martin, B. R. (1964) *Introduction to Biophysical Chemistry*, McGraw-Hill, New York.

McLaughlin, S. A. (1977) *Curr. Top. Membr. Transp. 9*, 71–144.

McLaughlin. S. A. (1989) *Annu. Rev. Biophys. Chem. 18*, 113–136.

Mutter, M., & Hersperger, R. (1990) *Angew. Chem. Int. Ed. Engl. 29*, 185–187.

Otvos, L., Szendrei, G. I., Lee, V. M. Y., & Mantsch, H. H. (1993) *Eur. J. Biochem. 211*, 249–257.

Rink, H. (1987) *Tetrahedron Lett. 28*, 3787–3790.

Rolka, K., Erne, D., & Schwyzer, R. (1986) *Helv. Chim. Acta 69*, 1798–1806.

Rueger, M., Bienert, M., Mehlis, B., Gast, K., Zirwer, D., & Behlke, J. (1984) *Biopolymers 23*, 747–758.
Seelig, A. (1990) *Biochim. Biophys. Acta 1030*, 111–118.
Seelig, A. (1992) *Biochemistry 31*, 2897–2904.
Seelig, A., & Macdonald, P. M. (1989) *Biochemistry 28*, 2490–2496.
Seelig, J., & Ganz, P. (1991) *Biochemistry 30*, 9354–9359.
Seelig, J., Nebel, S., Ganz, P., & Bruns, C. (1993) *Biochemistry 32*, 9714–9721.
Selkoe, D. J. (1993) *Trends Neurosci. 16*, 403–409.
Smithrud, D. B., Wyman, T. B., & Diederich, F. (1991) *J. Am. Chem. Soc. 113*, 5420–5426.
Terzi, E., Hölzemann, G., & Seelig, J. (1994) *Biochemistry 33*, 1345–1350.
Williams, R. W., & Weaver, J. L. (1990) *J. Biol. Chem. 265*, 2505–2513.
Wiseman, T., Williston, S., Brandts, J. F., & Lung-Nan, L. (1989) *Anal. Biochem. 179*, 131–137.
Yankner, B. A., Duffy, L. K., & Kirschner, D. A. (1990) *Science 250*, 279–282.